Orientation-switching transition and ferroelectricity in betaine arsenate

2009 J. Phys.: Condens. Matter 21 325901

(http://iopscience.iop.org/0953-8984/21/32/325901)

J. Phys.: Condens. Matter **21** (2009) 325901 (8pp) doi:10.1088/0953-8984/21/32/325901

Orientation-switching transition and ferroelectricity in betaine arsenate

J L Ribeiro, T Dekola and L G Vieira

Centro de Física da Universidade do Minho, Campus de Gualtar, 4715-057 Braga, Portugal

E-mail: jlr@fisica.uminho.pt

Received 28 April 2009, in final form 1 June 2009
Published 13 July 2009
Online at stacks.iop.org/JPhysCM/21/325901

Abstract

This paper reports a detailed investigation of the low frequency dielectric relaxation of betaine arsenate near the ferroelectric phase transition. The dielectric relaxation data are complemented with polarized infrared reflectivity data taken at low temperatures. The reported results allow us to identify several low frequency modes that clarify the complex behaviour of the dielectric response near the Curie temperature $T_{c2} \approx 120$ K. It is suggested that the important slow dynamics observed is linked to the reorientation of the betaine molecular group. The roles of the different molecular units in the structural changes are briefly discussed and a new and more complex phase transition sequence is proposed.

1. Introduction

Organic molecular crystals often display complex lattice dynamics that result from the existence of several nearly overlapping low energy phonon branches with rather flat dispersion relations. In addition, it often happens that the orientations of some molecular groups are driven by weak forces and give rise to order–disorder relaxations. For these reasons, cooperative phenomena and critical behaviour, if found in this type of crystal, may involve a complex interplay of several competing order parameters and interactions that can hardly be classified in the limiting cases of simple order–disorder or displacive mechanisms.

Betaine arsenate (hereafter denoted as BA; $(CH_3)_3NCH_2COOH_3AsO_4$) is a peculiar molecular ferroelectric known since 1982 [1]. It belongs to a group of mixed organic–inorganic compounds of the amino acid betaine that have been synthesized and widely investigated in the last decades [2]. At high temperatures, i.e. $T > T_{c1} = 411$ K, the crystals are orthorhombic [3]. Below T_{c1} and down to $T_{c2} = 120$ K crystals show a pseudo-orthorhombic morphology with two types of domains possessing monoclinic symmetry ($P12_1/n1$) [4]. As these domains can be reversed by a mechanical stress, this phase is ferroelastic. In this paraelectric and ferroelastic phase, the crystal structure consists of (100) sheets of parallel quasi-one-dimensional [001] chains of arsenate tetrahedra linked by strong hydrogen bonds. The betaine molecules are directed mainly along [100] and are attached to the tetrahedra by two weaker hydrogen bonds [4]. The ferroelastic domains share the same lattice constants but have slightly different monoclinic angles of $\beta = 91.23°$ and 88.77°. The domain walls are oriented parallel to the (001) and (100) planes.

Below $T_{c2} \sim 120$ K, the material becomes ferroelectric with a spontaneous polarization in the XZ plane, P_x being at least one order of magnitude smaller than P_z [1]. In this lower temperature phase, the material is an elasto-electric multiferroic. Structural x-ray data provide clear evidence for the loss of the two-fold symmetry axis, a necessary condition for the onset of spontaneous polarization in the XZ-plane [5]. The ferroelectric phase transition in BA is usually viewed as resulting from an order–disorder process in the bistable hydrogen bonds linking the arsenate tetrahedra. This picture has been established mainly from the early observation of a relaxational Debye type soft mode in the GHz frequency range which was assigned to proton ordering along the inorganic chains [6].

In spite of the extensive investigations carried out on BA, there remain several questions regarding its phase diagram that have been unanswered or unsatisfactorily interpreted. For example, a few degrees above T_{c2}, the polarization versus electric field hysteresis loops are strongly non-linear (consisting of S-shaped curves) [7] and a cross-over between a $d = 2$ Ising and a mean field or classical regime is observed in the critical behaviour of $\varepsilon_c(T)$ [8]. Also, the saturation of the electric polarization near T_{c2}—10 K (as seen from hysteresis loop measurements) is marked by an anomalous increase of the heat capacity [9]. The pyroelectric coefficient measured along the c-axis shows two anomalies in

the range 110–120 K, the second one marking a cross-over between two critical regimes in the temperature dependence of the spontaneous polarization [10]. The dielectric loss shows anomalies in the range 40–50 K whose origin has never been fully elucidated [11].

These features suggest that the onset of the ferroelectric phase in BA may involve mechanisms that are more complex than the simple ordering of the proton pseudo-spins. This is also suggested by the peculiar effects induced by deuteration or by the partial replacement of arsenate by phosphate. A deuteration content larger than 77% induces an unexpected complex phase sequence [12, 13] that includes the stabilization of an antiferroelectric and three iso-structural ferroelectric phases. Similarly, the partial replacement of arsenate by smaller phosphate ions [4, 14–16] stabilizes an antiferroelectric order to a surprisingly high concentration of the ferroelectric partner BA [17–20]: even for a ratio of BA to betaine phosphate (BP) of 3:1 the material becomes antiferroelectric and the antiferroelectric order does not coexist with any form of ferro or ferrielectric response [20]. Large ferroelectric domains of BA origin do not form in these solid solutions.

For these reasons, our interest in the investigation of this organic crystal was renewed. In a separate paper we reported an investigation of its phase transition sequence [21] with a polarized infrared reflectivity technique that allowed us to discriminate the angular orientation of the transition dipole related to the B_u polar phonons [22–24]. The results obtained in this study showed that at least four separate temperature regions could be identified close to T_{c2} (80 K $< T <$ 121 K), in which large molecular reorientations occur. Moreover, at lower temperatures ($T \sim 40$ K), the spectroscopic data provided evidence for some anomalies in the temperature dependence of some vibrational parameters. In the present work, we extend these studies with detailed low frequency dielectric relaxation measurements, complemented with new polarized infrared reflectivity data taken at low temperatures. The results reported allow us to identify several low frequency modes that clarify the complex behaviour of the dielectric response near T_{c2}, reveal the existence of an important slow dynamics linked to the reorientation of large molecular units and disclose evidence of an additional structural phase transition at lower temperatures. The roles of the different molecular units in these structural changes will be briefly discussed and a new and more complex phase transition sequence proposed.

2. Experimental details

The crystals of BA used in this work were grown by A Klöpperpieper (University of Saarbrücken) from equimolar aqueous solutions of betaine $(CH_3)_3NCH_2COO$ and As_2O_5. Large single crystals of monoclinic symmetry ($P2_1/n$) and good optical quality were oriented and samples cut and optically polished as (001) and (100) plates. Gold electrodes were deposited by sputtering. The samples were mounted in a closed cycle helium cryostat equipped with a programmable temperature control. The complex permittivity along the a- and c-axes was measured with an impedance analyser (Wayne–Kerr 6440A) working in the frequency range of 100 Hz–3 MHz. The dispersion was measured at a constant temperature (stability better than 0.1 K) by a computer controlled scanning of 45 frequencies in the available experimental window. At each temperature, the frequency was swept over repeated cycles in order to check the reproducibility of the measurements. The ac-measuring field was kept at a constant value of 600 V m^{-1}.

We took into account and analysed simultaneously the dispersion along the a- and the c-axes in the monoclinic plane. The dispersion of the complex permittivity was obtained from fitting the data to a sum of Havriliak–Negami functions [25, 26]:

$$\varepsilon(\omega) = \varepsilon' + \mathrm{i}\varepsilon'' = \varepsilon_\infty + \sum_j \Delta\varepsilon_j \left[1 + \mathrm{i}\left(2\pi \frac{\omega}{\Omega_j}\right)^{1-\alpha}\right]^{-\beta} \tag{1}$$

where ε_∞, $\Delta\varepsilon_j$, Ω_j, α_j and β_j are adjustable parameters: ε_∞ is the permittivity at infinite frequency, $\Delta\varepsilon_j$ and Ω_j the strength and frequency of the jth relaxational mode, respectively. The parameters α_j and β_j control, respectively, the width and symmetry of the distribution of the dielectric relaxation time of the mode. The real and imaginary components of $\varepsilon(\omega)$ were simultaneously fitted to ensure compatibility with Kramers–Kronig inversion.

For the infrared measurements, parallelepiped samples were cut and optically polished, with the major faces oriented perpendicular to the monoclinic b-axis. The polarized infrared reflectivity spectra were measured at near normal incidence with a Bruker IFS 66V spectrometer and a closed cycle helium cryostat (18–300 K). The average angle of incidence was about 11°. A set of different light sources, beamsplitters, polarizers and detectors were used to cover the frequency range 40–4000 cm^{-1}. In the middle infrared range (500–4000 cm^{-1}) we used a global source, a KBr beamsplitter, a KRS-5 polarizer and a DTGS:KBr detector. The far infrared region was studied with a Hg lamp, a 6 μ-M8 Mylar beamsplitter, a polyethylene polarizer and a DTGS-PE detector. The reference spectra for calibration of the absolute reflectivity were registered with a gold mirror for each of the polarization directions used and the instrumental resolution was better than 2 cm^{-1} over the whole frequency range investigated. The polarizers were mounted in the optical path of the incident beam.

We measured the reflectivity at near normal incidence in the ac-plane with light polarized along the c-axis and evaluated the complex dielectric function $\varepsilon_c\ (\omega, T)$ from Kramers–Kronig inversion of the reflectivity. As shown in [21], because of the pseudo-orthorhombic symmetry of the crystal, the use of this method to evaluate the dielectric function is reliable at least for frequencies higher than 500 cm^{-1}.

3. Experimental results

As referred to above, the order–disorder character of the ferroelectric phase transition in BA has been established from high frequency dielectric measurements (0.1 MHz–10 GHz) performed in the temperature range above $T = 115$ K [6]. In the case of the protonated compound, these authors have detected in the paraelectric phase a mono-dispersive relaxational soft mode with a frequency that

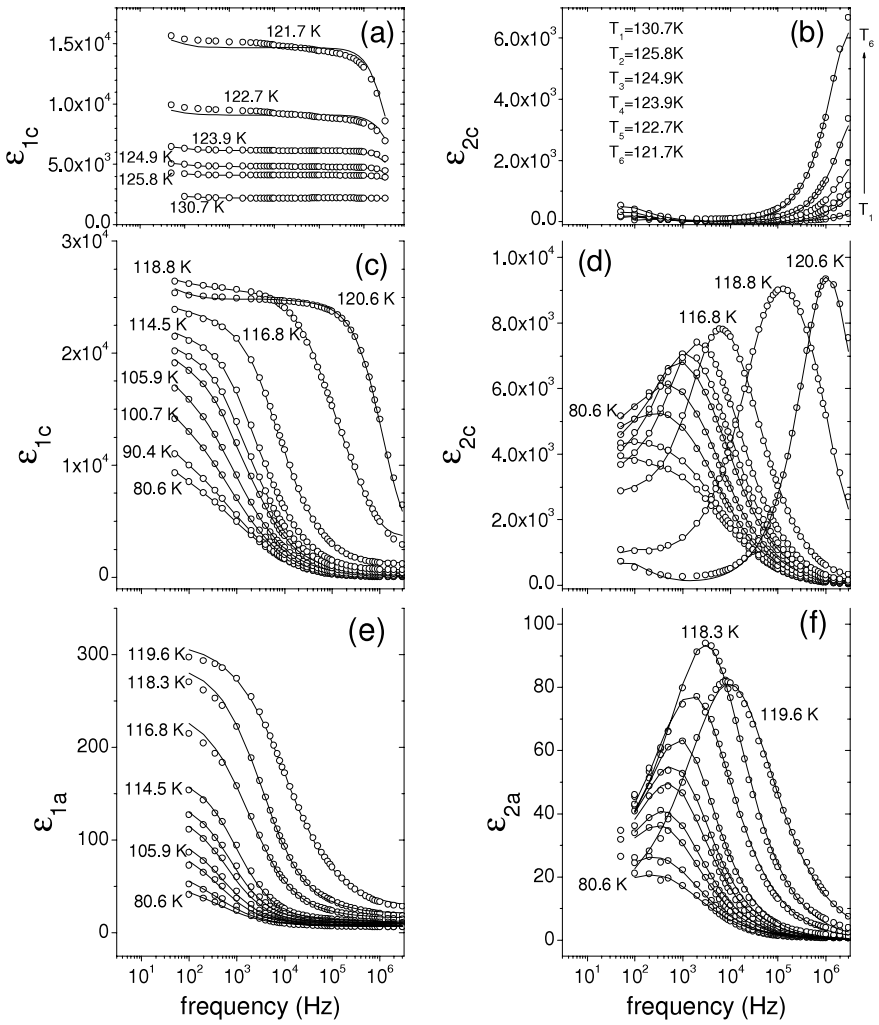

Figure 1. Real (ε_1) and imaginary (ε_2) components of the permittivity measured along [001] (a–d) and [100] (e, f) in the frequency and temperature ranges of 10–3 $\times$ 10^6 Hz and 80–130 K, respectively. The solid lines were calculated from the best fit of the model function (1) to the data.

decreases almost linearly with temperature as $T \rightarrow T_{c2}$ from above. The value of ε_∞ was found to be unusually high and was strongly temperature dependent, indicating that other cooperative mechanisms should be considered. An additional relaxational soft mode was revealed from the sub-millimetre backwave oscillator response (10^{11} Hz) at room temperature, but its temperature dependence was not reported [27].

An earlier study [28] of the dielectric dispersion in the ferroelectric phase, along the *c*-axis, allowed the detection of two temperature dependent relaxations below T_{c2}. However, the number of temperatures and frequencies considered was scarce, especially at low temperatures and low frequencies: no data have been reported below 5 kHz and $T < 60$ K.

Let us consider first the dispersion observed close to T_{c2}. Figure 1 shows the real and imaginary components of the dielectric function measured along [001] (figures (a)–(d)) and along [100] (figures (e) and (f)). As seen, in the paraelectric phase, we detect close to T_{c2} a soft relaxational mode (m_{1c}) that enters the experimental frequency window near $T =$ 130 K. This mode is polarized along the *c*-axis, is of a Debye type ($\alpha = 0$, $\beta = 1$) and its strength increases markedly on approaching the Curie temperature. In the paraelectric phase ($T > T^* = 121$ K), the temperature dependence of the frequency of the mode m_{1c} can be well fitted to the Eyring equation ($\nu \propto \frac{e^{-\frac{\Delta U}{k_B T}}}{T}$, ν being the frequency of the mode), giving an activation energy of the potential barriers of $\Delta U \approx 126$ meV. Below $T \sim T^*$, this mode becomes polydispersive ($\alpha \approx 0.15$) and asymmetric ($\beta \approx 0.9$). For $T < T_{c2} = 119$ K, the data are better fitted by assuming two separate higher frequency modes (labelled as m_{1c} and m_{2c}) than by considering a single and strongly asymmetric mode (see comparison in figure 2(e)). The frequency of these two modes decreases very steeply on cooling further to $T^{**} =$ 110 K. In addition, we detect a low frequency mode (100 Hz) that has a nearly constant frequency and a weak strength over the whole temperature range investigated (mode m_{3c}).

Along the [100] direction, the dielectric function shows no detectable dispersion in the experimental frequency range down to T^*. Near T_{c2}, we detected the appearance of a strongly polydispersive ($\alpha \approx 0.35$) and symmetric ($\beta \approx 0.99$) mode. Below T^{**}, the frequency of this mode (m_{1a}) matches that of

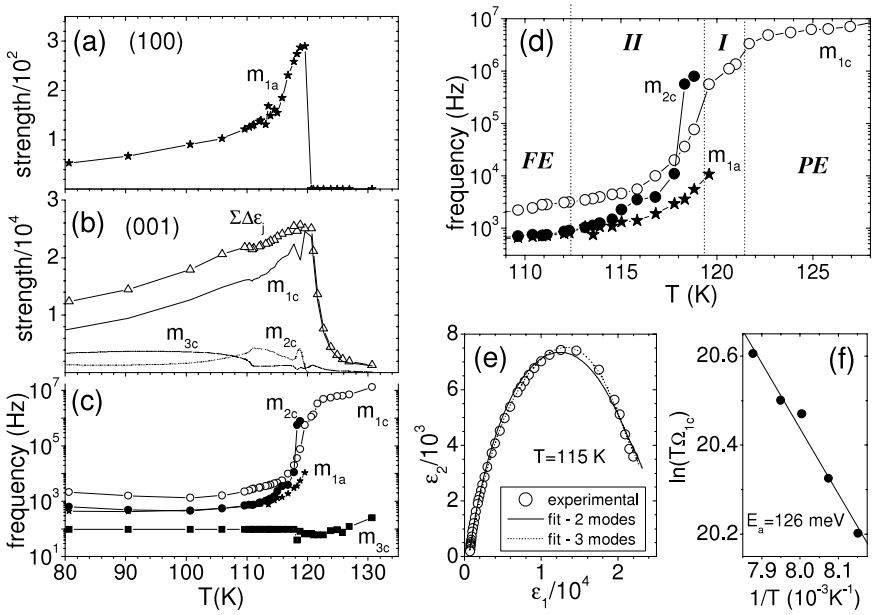

Figure 2. Temperature dependence of the dielectric strength of the relaxational modes detected in the frequency range 10–3 $\times$ 10^6 Hz along the [100] (a) and [001] (b) crystallographic axes. The temperature dependence of the frequency of the different modes is shown in (c) (20–130 K) and (d) (a detail of the range 110–130 K). (e) The Cole–Cole plot of the data measured at 115 K and the corresponding best fits considering, besides the lower frequency mode m_{3c}, one or two higher frequency modes (see text). The Eyring plot of the frequency of m_{1c} in the paraelectric phase is shown in (f).

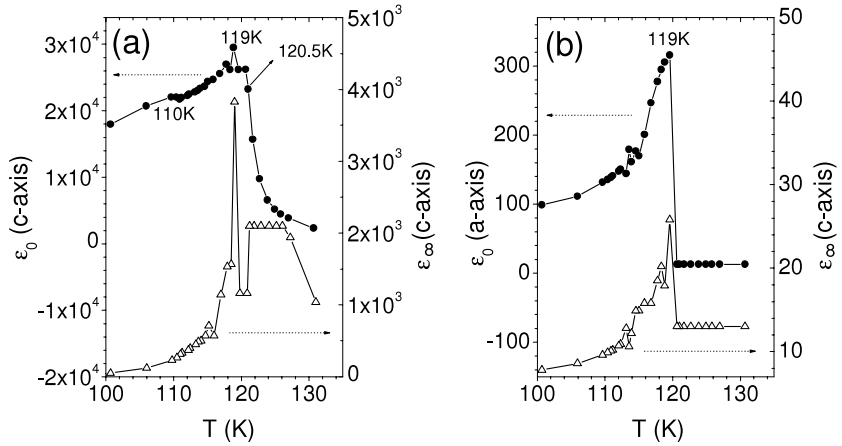

Figure 3. Temperature dependence of the permittivity in the limiting cases of zero and infinite frequency, as obtained from fitting the data to equation (1). The behaviour shows that there exists at least an additional relaxation at higher frequencies that shows a critical behaviour close to T_{c2}. The strength of such a mode vanishes below about $T = 110$ K. Two anomalies are clearly seen at 119 and 110 K in the static permittivity.

the mode m_{2c} found along the c-axis but differs substantially from it above this temperature (see figures 1(d) and (f)). This a-polarized mode cannot be seen as a projection of the soft mode m_{1c} caused by a misfit of the orientation of the sample. This conclusion results directly from the different frequencies of the two modes at a given temperature. The mode detected along the a-axis is therefore separate from the principal soft relaxational mode seen in the paraelectric phase.

Figure 2 shows the temperature dependence of the frequency of the different modes detected over the temperature range 80–140 K, together with their dielectric strength contributing to the static permittivity. Close to T_{c2}, the static dielectric response is mainly driven by the primary mode m_{1c}. The strength of this mode shows two separate maxima at about $T^* = 121$ K and $T_{c2} = 119$ K, along with a shoulder at about $T^{**} = 110$ K. On the other hand, the strength of the mode m_{2c} displays a relative maximum at about T^{**} ($\Delta\varepsilon \approx 4500$). Along the a-axis, the mode m_{1a} has a strength ($\Delta\varepsilon \approx 300$ at T_{c2}) that decreases monotonically on further cooling from T_{c2}.

It is interesting to compare the temperature dependence of the permittivity in the limiting cases of zero (ε_0) and infinite frequency (ε_∞) (figure 3). In agreement with previous results [6], the high frequency permittivity ε_∞ along the c-axis shows pronounced temperature dependence, unusual

high values in the paraelectric phase ($\sim 10^3$) and a sharp peak at $T_{c2} = 119$ K. Below this temperature, its value decreases sharply and reaches 'normal values' below 100 K. Similarly, a maximum at T_{c2} is detected in the value of ε_∞ measured along the a-axis. The marked temperature dependences of these high frequency parameters indicate clearly the existence of other higher frequency relaxations displaying a critical behaviour near T_{c2}. This conclusion is consistent with the previous detection of a temperature dependent central mode by Raman and infrared spectroscopy [21, 29, 30].

The permittivity in the limit $\omega \to 0$, ε_0, is also shown in figure 3. It corresponds to the sum of ε_∞ with the strengths of the different modes. The interpretation of the temperature dependence of the dielectric function near the critical region, when measured at a finite frequency, is hampered by the strong dispersion observed because the details of the function strongly depend on the frequency employed. Here, however, we have a 'static limit' that reflects the quasi-equilibrium response of the polarization to the applied measuring field. The value of ε_0 along the c-axis shows clear anomalies at $T^* = 121$, $T_{c2} = 119$ K and $T^{**} = 110$ K, while a single anomaly at $T_{c2} = 119$ K is seen in ε_0 for fields applied along the a-axis. From these results we can identify two temperature ranges that correspond to the paraelectric ($T > T^* = 121$ K) and the ferroelectric phases ($T < T^{**} = 110$ K). Sandwiched between these two phases, we can identify two intermediate temperature regions that we denote as region-I ($T_{c2} = 119\,\text{K} < T < T^*$) and region-II ($T^{**} < T < T_{c2}$). This set of four temperature ranges can also be delimited by the inspection of the temperature dependence of the frequency of the modes m_{1a}, m_{1c} and m_{2c}, shown in more detail in figure 2(d).

In the temperature range of region-I, the mode m_{1c} softens abruptly. It is interesting to note that this temperature region corresponds to the range where the polarization versus electric field hysteresis curves, taken at the frequency of 1 Hz, show closed S-shaped forms that reflect a strongly non-linear response of the polarization to the electric field [7]. Since no ferroelectric loops are observed here, we will denote this region as the non-linear paraelectric region (NLP). In the intermediate region-II, the hysteresis loop measurements with a Sawyer–Tower circuit without loss compensation show strongly distorted loops under weak applied fields [1, 7]. These distortions depend on the amplitude of the field and vanish only under ac fields of high amplitude [1, 7]. It has been shown that the dielectric response in this temperature range is very strongly dependent on the bias field and on the amplitude and frequency of the measuring ac field [31]. This behaviour is similar to that found in some disordered polar dielectrics and suggests that a certain degree of disorder is present in the system [29]. This hypothesis is reinforced by early pyroelectric and x-ray data that revealed that the electric polarization measured at zero field (zero field cooling polarization) is small (5.7×10^{-4} C m^{-2}) if compared with that measured at a moderate field of 200 V cm^{-1} (240×10^{-4} C m^{-2}) [30], and that the correlation length of the polar domains increases near T_{c2}, thus creating some local ordering of the system, but remains at the rather low value of $\xi \approx 300$ Å [5]. Note that this correlation length corresponds approximately to polar regions of about 30 unit cells. We therefore have ample evidence that immediately below T_{c2}, and in the intermediate temperature region-II, the system remains in a disordered multidomain state.

In the dielectric relaxation data, the symmetry breaking at T_{c2} is clearly marked by the appearance of two additional low frequency modes, m_{2c} and m_{1a}. Initially, these two modes have distinct frequencies but, on cooling, their values merge to a common value (see figure 2(d)). Curiously, this happens near T^{**}, a temperature that is signalled by anomalies in the static dielectric response (figure 3) and is detected in the lattice heat capacity [32]. This temperature also marks the appearance of normal ferroelectric loops (whose form is neither distorted nor depends on the amplitude of the field) [7].

The merging of the frequency of the modes m_{2c} and m_{1a} to a common value, occurring near T^{**}, looks like an inverted branching process in which a single mode seen at lower temperatures splits, at higher temperatures, into two different modes. This type of mode branching often signals in the spectroscopic data the occurrence of an order–disorder process. Therefore, the observed merging of the frequencies of the modes m_{2c} and m_{1a} may indicate that a transition from a non-homogeneous and multidomain state to a more homogeneous dipolar order occurs at about T^{**}.

Let us now consider the lower temperature range. The frequency and temperature dependence of the real and imaginary components of the dielectric function measured along the c- and a-axis in this lower temperature range is shown in figure 4. Below $T \approx 80$ K, it becomes increasingly difficult to adequately fit the experimental data because both the lower frequency plateau in the permittivity and the location of the maximum in the loss spectrum progressively move to outside the frequency window, on cooling. The experimental values of the permittivity and loss remain, however, anomalously high down to temperatures of the order of $T_3 \approx 40$ K. Below this temperature their values decrease very steeply. This change is accompanied by the detection of two additional relaxational modes, polarized along the a-axis (mode m_{2a}) and along the c-axis (mode m_{4c}), respectively. This can be more clearly seen in the insets of figure 4.

Below $T \sim T_3$, the modes m_{2a} and m_{4c} coexist with the other relaxations found at higher temperatures. We cannot entirely rule out the possibility of these new modes just being hidden at higher temperatures by the stronger dielectric strengths of other modes. However, the fact that their frequencies are strongly dependent on temperature and the coincidence of their appearance with the steep decrease observed in the permittivity, suggest that some structural change may occur in this temperature range. In order to help further elucidate this point, we monitored in detail the low temperature behaviour of the polar vibrational modes by measuring the infrared reflectivity of incident light polarized along the polar c-axis.

Figure 5 shows the frequency and temperature dependence of the imaginary part of the dielectric function in three different infrared spectral regions. The first frequency range (figure 5(a)) corresponds to that of the internal vibrations ν_1

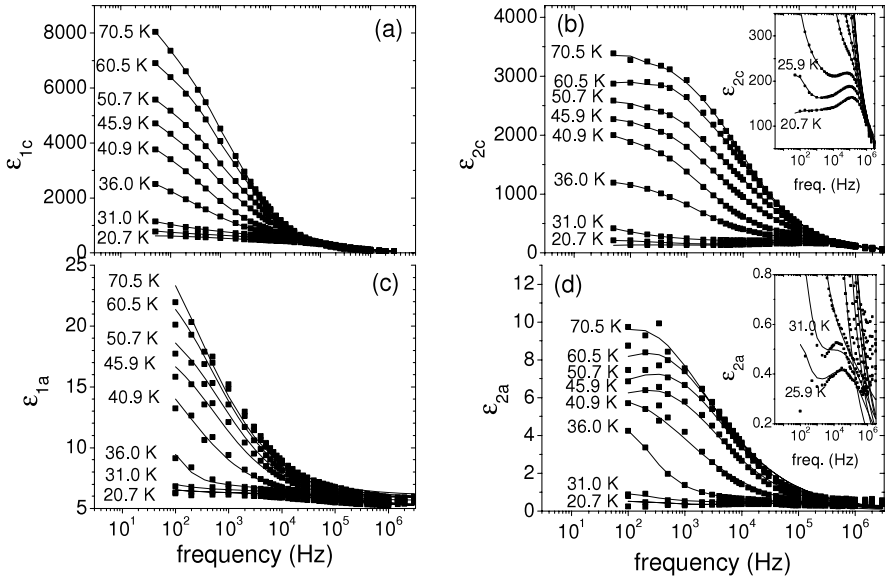

Figure 4. Detail of the real and imaginary components of the permittivity measured along the [001] (a, b) and [100] (c, d) in the frequency and temperature ranges of 10–3 × 10^6 Hz and 20–80 K, respectively. The insets shows in more detail the new modes detected at low temperatures.

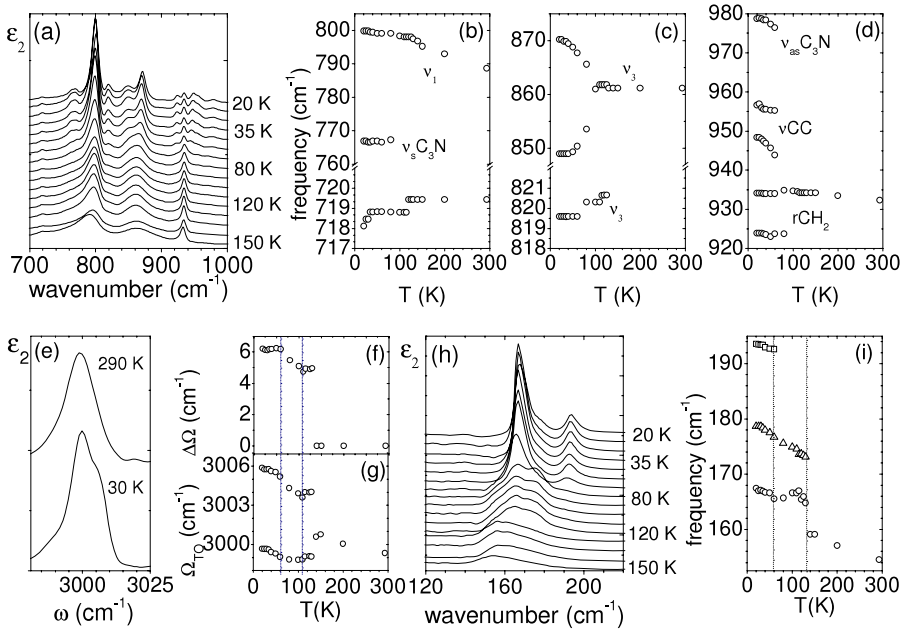

Figure 5. Detail of the real and imaginary components of the permittivity obtained from Kramers–Kronig inversion of the reflectivity data (see text) in three different spectral ranges. The temperature dependence of the frequency of several modes is also shown.

(790 cm^{-1}), ν_3' (862 cm^{-1}) and ν_3'' (820 cm^{-1}) of the arsenate tetrahedron and the internal modes of the betaine molecule $\nu_{as}C_3N$ (978 cm^{-1}), ν_sC_3N (790 cm^{-1}), νCC (960 cm^{-1}) and rCH$_2$ (934 cm^{-1}) (for a detailed assignment of the vibrational modes see [21]). Here, several new modes of the betaine molecule may be seen at lower temperatures ($T < 60$ K) in the frequency range corresponding to the rCH$_2$ and the νCC modes (see figures 5(b) and (d)). This spectral change is consistent with either a reorientation or a deformation of the betaine molecule. Also interesting is the behaviour of the internal mode ν_3' of the arsenate ion, located near 860 cm^{-1}. As seen, at T_{c2} this mode splits into two components due to the appearance of two non-equivalent sets of arsenate ions. On further cooling, the difference in frequency between these components continuously increases down to $T \sim T_3$ but remains nearly constant below this temperature. A similar behaviour is observed in the temperature dependence of the stretching mode of the methyl group located near 3000 cm^{-1} (figures 5(e)–(g)). Here, at T_{c2}, the band also splits into two components, whose separation in frequency increases continuously between 110 and 50 K. Below this latter temperature this separation reaches a constant plateau.

Finally, the lattice modes located in the frequency range 160–195 cm^{-1} also show important spectral changes (see figures 5(h) and (i)). These changes, seen not only

near T_{c2} but also near T_3, suggest that modifications of the relative molecular orientations of the betaines and the arsenate tetrahedra occur near 50 K. Structural studies in this temperature range might further elucidate these points.

4. Discussion and conclusion

The above results show that the phase sequence in BA is complex. From the spectroscopic data, at least five different temperature ranges can be delimited below room temperature: the paraelectric phase ($T > T^* = 121$ K), the non-linear phase ($T_{c2} = 119$ K $< T < T^*$,), the disordered or multidomain ferroelectric phase $T^{**} = 110$ K $< T < T_{2c}$, the ferroelectric phase $T_3 \sim 40$ K $< T < T_3$ and a low temperature phase $T < T_3$.

Above T_{2c}, the material displays (along the c-axis) linear ($T > T_1$) or S-shaped ($T_1 > T > T_2$) closed polarization versus electric field curves [7]. This transition from a linear to a strongly non-linear paraelectric response is signalled in the dielectric relaxation data by a steeper softening of the frequency of the primary mode m_{1c}, which is polarized along the c-axis. This transition appears to result from the formation of dynamical clusters exhibiting strong polar short range and dynamical order, similar to that found in a superparaelectric [20], and is also marked by a sharp increase of the non-linear permittivity [10, 33].

The symmetry breaking at T_{2c}, related to the onset of ferroelectricity, is seen in the relaxational data by the appearance of two additional relaxational modes, m_{2c} and m_{1a}, polarized along the [001] and [100], respectively. The frequencies of these two modes decrease on cooling and merge together at a common value near T^{**}. The mode m_{1a} is distinct from the primary mode m_{1c} and is responsible for the anomaly observed in ε_a at T_2. This suggests that the component of the polarization along this axis, P_a, may result from the ordering of separate molecular units. Given its strong dipolar moment it seems plausible that the betaine molecules may play an important role here.

The transition from the disordered or multidomain phase to the ferroelectric phase, at $T^{**} = 110$ K, could originate from an orientation-switching mechanism [34]. This kind of structural transformation can be found in complex molecular crystals and it may happen when the orientation of large molecular units, either in a plane or in three dimensions, is controlled by weak forces. The ordering of a small group of atoms via an order–disorder mechanism (in the present case, the protons linking the arsenate ions) may trigger a spatial reorientation of the larger units. These reorientations may be locally fast but the degree of disorder is a continuous function of the temperature and a finite temperature interval may be needed to complete the change from a state involving disorder to a state without the wrong molecular orientations. In the case of BA the obvious candidates for such a process of orientation switching are the betaine molecules.

In fact, the rotational thermal amplitudes (librations) of the betaine molecules are large [4], and alternative orientations of not much greater energy are possible. This means that the probability of 'wrong' orientations may be high immediately below T_{2c}. Each 'wrong' betaine molecule displaces its immediate neighbours slightly, which, in turn, influences the orientation of the next molecule. The crystal as a whole would divide into small ordered polar and piezoelectric domains with rapidly shifting boundaries. The pattern of these domains would be strongly dependent on the temperature, electric and stress fields.

In an orientation-switching transition, the orientation of the 'average molecule' changes continuously with temperature. This change may give rise to detectable anomalies in the lattice specific heat or the thermal expansion curves [34]. It also produces important changes in the orientation of the transition dipoles of the lattice modes and internal molecular vibrations. The existence of such molecular reorientations in BA has been recently investigated in detail by analysing the polarized infrared reflectivity spectra of incident light polarized along different directions in the monoclinic plane [21]. This study, by showing that the transition dipoles of several vibrational modes related to the betaine and arsenate groups rotated steeply immediately below T_{c2}, provided compelling evidence for the existence of such a mechanism in BA.

Can this orientation-switching transition revealed by infrared reflectivity explain the merging of the frequencies of the relaxational modes m_{2c} and m_{1a}? There is evidence for the existence in BA of strong short range ferroelectric interactions in two dimensions, probably occurring in the XZ layers formed by the arsenate ions, together with competing weak short range antiferroelectric and long range ferroelectric couplings along the third direction. The balance of the later competing interactions may be influenced by deuteration, the size of the inorganic tetrahedra (as in the case of the arsenate or phosphate systems) or the orientation of the betaine molecules. A certain degree of disorder in this molecular group may favour a stabilization of a pattern of ferroelectric domains with domain walls roughly oriented perpendicular to the a-axis. Given the piezoelectric coupling allowed by symmetry within each domain ($p_3 = d_{35}e_5$), this structure would result in a strong anisotropic stress field that could give rise to the different frequencies of the modes m_{2c} and m_{1a}. The progressive ordering of the orientation of the betaine molecules would give rise to an increase of the width of the ferroelectric domains and a subsequent decrease of the domain wall density and intensity of the stress field. As a result, the frequency of the modes m_{2c} and m_{1a} would progressively merge into a common value, reflecting the progressive onset of a more homogeneous ferroelectric order. Note that, if the domain pattern stabilized just below T_{c2} has a long range order, this conjectured evolution would correspond to the stabilization of a long-period (squared) polarization wave, with a temperature dependent wavenumber. This intermediate phase could help to explain not only the high values of the permittivity that are observed experimentally but also the remarkable stability of the antiferroelectric order in BA–BP solid solutions. Further structural investigations are needed to clarify this possibility.

The reorientation of the organic molecular group is a thermally activated process that could, in principle, induce in the system a non-ergodic behaviour. This ergodicity breaking would give rise, for example, to an important thermal

hysteresis or time dependence of the permittivity measured at a constant temperature. The thermal hysteresis experimentally observed in the location of the maximum of the permittivity between heating and cooling runs, at a rate of 1 K min^{-1} is, however, rather small (<0.5 K). Also, over the time needed to measure the frequency dependence of the permittivity at a given temperature (about 45 s due to the repeated frequency cycles and the stabilization time allowed between measurements at different frequencies), no meaningful change of the permittivity was detected. This indicates that if a time dependence of ε exists, particularly in the intermediate region-II, it must involve small relaxation amplitudes or long timescales.

The homogeneous ferroelectric phase stabilized below T^{**} has a monoclinic symmetry [5]. This means that the orientation of the transition dipoles that lie in the monoclinic plane is not fixed by symmetry and their orientation may vary with the temperature. This allows for a slow and cooperative reorientation of certain molecular units as the temperature is lowered. This type of continuous molecular change could eventually induce distortions in certain molecular units, producing the symmetry breaking that is apparent at low temperatures in the dielectric relaxation and infrared data. This mechanism could account for the stabilization of the flat hysteresis loop phase observed in BA–BP solid solutions [20].

Acknowledgment

The authors wish to thank Dr A Klöpperpieper (University of Saarbrücken) for supplying the crystals used in this work.

References

[1] Klöpperpieper A, Rother H J, Albers J and Ehses K H 1982 *Ferroelectr. Lett.* **44** 115
[2] Schaack G 1990 *Ferroelectrics* **104** 147
[3] Hayase S, Koshiba T, Terauchi H, Maeda M and Suzuki I 1989 *Ferroelectrics* **96** 221
[4] Schildkamp W, Schäfer G and Spilker J 1984 *Z. Kristallogr.* **168** 187
[5] Moreira J A, Kiat J M, Chaves M R, Almeida A and Klöpperpieper A 2000 *Phys. Status Solidi* a **178** 633
[6] Freitag O, Bruckner H J and Unrhu H G 1985 *Z. Phys.* B **61** 75
[7] Müser H E and Schell U 1984 *Ferroelectrics* **55** 279
[8] Schell U and Müser H E 1987 *Z. Phys.* B **66** 237
[9] Frühauf K P, Sauerland E, Helwig J and Müser H E 1984 *Ferroelectrics* **54** 293
[10] Lacerda-Arôso M T, Ribeiro J L, Chaves M R, Almeida A, Vieira L G, Klöpperpieper A and Albers J 1994 *Phys. Status Solidi* b **185** 265
[11] Lanceros-Mendez S, Ebert H, Schaack G and Klöpperpieper A 2003 *Phys. Rev.* B **67** 014109
[12] Albers J, Klöpperpieper A, Müser H E and Rother H J 1984 *Ferroelectrics* **54** 45
[13] Almeida A, Simeão-Carvalho P, Chaves M R, Klöpperpieper A and Albers J 1994 *Phys. Status Solidi* b **184** 225
[14] Klöpperpieper A, Rother H J, Albers J and Ehses K H 1982 *Ferroelectr. Lett. Sect.* **44** 115
[15] Albers J, Klöpperpieper A, Rother H J and Ehses K H 1982 *Phys. Status Solidi* a **74** 553
[16] Albers J 1988 *Ferroelectrics* **78** 3
[17] Lanceros-Méndez S, Ebert H, Schaack G and Klöpperpieper A 2003 *Phys. Rev.* B **67** 014109
[18] Höchli U T, Knorr K and Loidl A 1990 *Adv. Phys.* **39** 405
[19] Manger M, Lanceros-Méndez S, Schaack G and Klöpperpieper A 1996 *J. Phys.: Condens. Matter* **8** 4617
[20] Almeida A, Sarmento S, Chaves M R, Ribeiro J L, Vieira L G, Santos M L, Klöpperpieper A and Costa A M 2006 *Phys. Rev.* B **74** 064112
[21] Ribeiro J L, Vieira L G, Dekola T and Tarroso-Gomes I 2009 *Vib. Spectrosc.* **50** 198
[22] Belousov M V and Pavinich V F 1978 *Opt. Spectrosc.* **45** 771
Pavinich V F and Belousov M V 1978 *Opt. Spectrosc.* **45** 881
Pavinich V F and Bochtarev V A 1988 *Opt. Spectrosc.* **65** 640
[23] Kuz'menko A B, van der Marel D, van Bentum P J M, Tishchenko E A, Presura C and Bush A A 2001 *Phys. Rev.* B **63** 094303
[24] Kuz'menko A B, Tishchenko E A and Orlov V G 1996 *J. Phys.: Condens. Matter* **8** 6199
[25] Havriliak S and Negami S 1966 *J. Polym. Sci.* C **14** 99
[26] Havriliak S and Negami S 1967 *Polymer* **8** 161
[27] Goncharov Yu G, Kozlov G V, Volkov A A, Albers J and Petzelt J 1988 *Ferroelectrics* **80** 221
[28] Almeida A, Agostinho Moreira J, Chaves M R, Klöpperpieper A and Pinto F 1998 *J. Phys.: Condens. Matter* **10** 3035
[29] Yuzyuk Yu I, Agostinho Moreira J, Almeida A, Chaves M R and Pinto F 2000 *Phys. Rev.* B **61** 15035
[30] Moreira J A, Almeida A, Chaves M R, Mota M F, Klöpperpieper A and Pinto F 1998 *J. Phys.: Condens. Matter* **10** 6825
[31] Almeida A, Carvalho P S, Chaves M R, Pires A R, Müser H E and Klöpperpieper A 1990 *Ferroelectrics* **108** 347
[32] Frühauf P, Sauerland E, Helwig J and Müser H E 1984 *Ferroelectrics* **54** 293
[33] Iwata M, Nagata T, Orihara H and Ishibashi Y 1996 *J. Korean Phys. Soc.* **29** S452 (Proc. Suppl.)
[34] Megaw H D 1973 *Crystal Structures: a Working Approach* (London: Saunders)